# DISCHARGE FORECASTS IN MOUNTAIN BASINS BASED ON SATELLITE SNOW COVER MAPPING

J. Martinec and A. Rango, Federal Institute for Snow and Avalanche Research, Weissfluhjoch/Davos, Switzerland and Goddard Space Flight Center, Greenbelt, Maryland, U.S.A.

## ABSTRACT

Depletion curves of the areal extent of snow cover are shown to be basic information in a snowmelt-runoff model. Originally developed in European mountain basins, the procedure is now applied to simulate the runoff in the Rocky Mountains with the use of the Landsat imagery and air temperature data. The method requires a proper assessment of the recession coefficient of discharge in a given basin. It is adaptable to operational short-term forecasts of discharge and to evaluation of seasonal runoff volumes.

## INTRODUCTION

It has long been recognized that the areal extent of snow cover in a basin is an important factor for determining the amount of snowmelt runoff produced in the spring. Attempts to measure the snow-covered area from the ground using oblique photography or visual observations have not been acceptable, especially in large basins, because of a lack of basin-wide measurements including those for hidden slopes and a poor observing perspective. As a result, aircraft have been employed to provide an improved observing capability for snow-covered area mapping. Because most flights are conducted at low altitudes, in cases where complete basin coverage is required, much of the photography is still necessarily oblique which causes significant locational problems and limits the approach to general snow cover estimates. An alternative approach using low altitude aircraft flights makes use of a previously drafted watershed base map and a snow cover observer (Warskow, Wilson, and Kirdar, 1975). In this method the observer records the visual location of the snowline on the base map as the flight passes over pre-selected ground areas. At the same time he may make estimates of snow depth and melting condition of the snowpack based on the appearance of ground features. After returning from a flight the data are processed and a snow-covered area map is produced.

Because earth-oriented vertical photographs taken from low altitudes cover only a relatively small area, they are limited to snow-covered area determinations on correspondingly small watersheds or index areas for larger basins. Snow-cover mapping with 1:6,000 scale aerial photography was found to produce useful data for snowmelt runoff simulation in the Colorado Rocky Mountains (Leaf, 1969; Haeffner and Barnes, 1972). As the aircraft altitude is increased, larger areas come into the field of view of the cameras and snow cover over increasingly large watersheds can be mapped. It has been shown by Martinec (1972) that photography from 8.5 km altitude could be used to repetitively map the snow cover of the 43.3 $km^2$ Dischma basin near Davos, Switzerland. The snow cover data thus

obtained was used in simulation of daily snowmelt runoff for the Dischma basin. When larger watersheds are encountered, however, more expensive and time consuming use of several photographs is necessary. Even from the altitude of the NASA U-2 aircraft (18.3 km), mosaicking of five photographs is required to cover the 228 km$^2$ Dinwoody Creek watershed in the Wind River Mountains (a part of the Rocky Mountains) of Wyoming, U.S.A. (Rango, 1977).

Figure 1 shows an orthophoto of the Dischma basin. In this typical alpine valley with rugged terrain, the snow cover consists of many scattered patches. In order to determine the areal extent of the snow as a percent of the total area, a computerized procedure was adopted which consists of counting the snow-covered

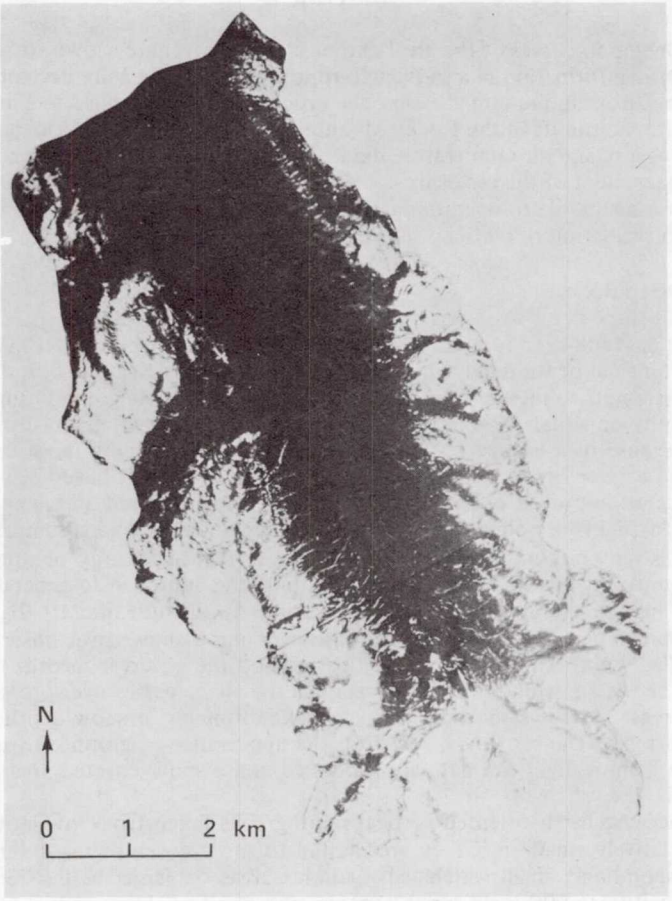


Fig. 1—Orthophotograph showing the snow cover in the Dischma basin (Swiss Alps) on 8 June 1976.

and snow-free points. Because about 215,000 points are counted within the watershed boundary, the effective resolution is about 15 m.

Figure 2 shows a simultaneous Landsat image which has been produced (Urfer, 1978) by digital classification of each pixel as snow-covered, partially snow-covered, or snow-free, respectively. The resolution of Landsat is entirely adequate for hydrological evaluations even in a basin of this relatively small size. For larger basins the use of Landsat eliminates the troublesome task of mosaicking several aerial photographs. Conversely, the periodic monitoring of the seasonal snow cover in the Alps is frequently disturbed by clouds.

## SNOW-COVER DEPLETION CURVES

The areal extent of snow cover constitutes basic information for the day-to-day computation of snowmelt runoff. The snow-covered area cannot reliably indicate the water volume stored in the snowpack, however, as illustrated by Figure 3. Although the snow coverage was similar on both dates, the water equivalent measured in a representative site was about 800 mm on June 22, 1970, and only about 410 mm on May 16, 1969. The snow coverage should probably be related to the ratio of the current snow depth, $H_{s\ actual}$, to the maximum snow depth of the

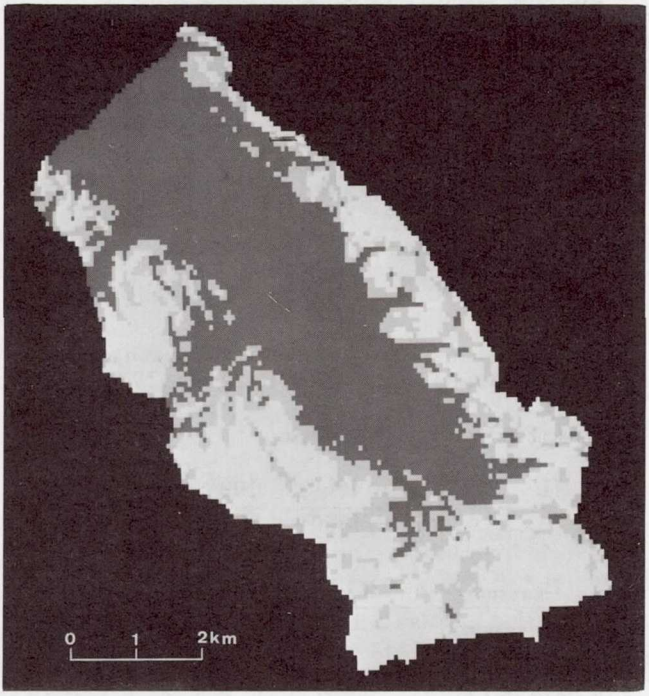


Fig. 2—Satellite image of the Dischma basin on 8 June 1976 with digitally classified snow cover evaluated from Landsat 2 data (reproduced by courtesy of the Department of Geography, University of Zurich, Switzerland).

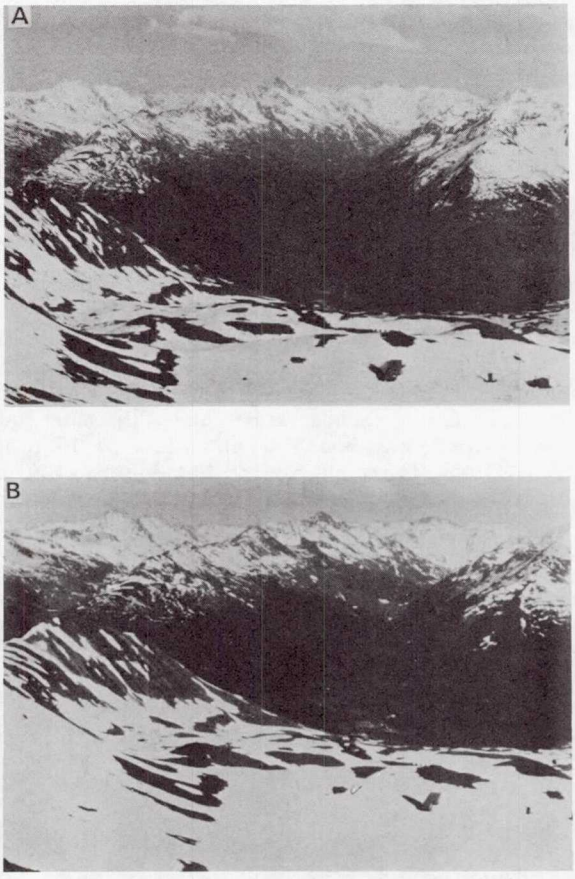


Fig. 3—Terrestrial photos of the Dischma basin and the vicinity, A) 16 May 1969, B) 22 June 1970.

respective winter season, $H_{s\,max}$. In this case,

$$\frac{H_{s\,actual}\,(\text{May 16, 1969})}{H_{s\,max}\,(\text{April 18, 1969})} = \frac{109\text{ cm}}{208\text{ cm}} = 0.524$$

$$\frac{H_{s\,actual}\,(\text{June 22, 1970})}{H_{s\,max}\,(\text{May 2, 1970})} = \frac{158\text{ cm}}{321\text{ cm}} = 0.492$$

Thus similar areal extents of the snow cover as shown in Figure 3 correspond to similar snow-depth ratios.

For seasonal discharge forecasts, it would be useful to replace snow depths by water equivalents. It remains to be seen whether such interpretations of the snow coverage can produce reasonably consistent relations. In any case, a short-lived

snow cover caused by occasional snow storms during the snowmelt season should be disregarded in these evaluations.

An example of depletion curves of the snow coverage in the Dischma basin is shown in Figure 4. In addition to the entire watershed, separate curves have been plotted for the three elevation bands A(1668-2100 m), B(2100-2600 m), and C(2600-3146 m), respectively. In Figure 5, depletion curves in the Dinwoody basin for four elevation bands (A:1981-2438 m, B:2438-2896 m, C:2896-3353 m, and D:3353-4202 m) show a different pattern of the snow cover retreat. The gradually rising snow line can be better defined than in Dischma, enabling photo interpretation and planimetering to be used with much greater ease.

## RUNOFF CHARACTERISTICS IN MOUNTAIN BASINS

During a snowmelt season, the seasonal increase of temperature is accompanied by a gradual diminution of the snow-covered area. This situation is shown in Figure 6. If the meltwater volume is a product of the energy input (represented by degree-days) and of the snow-covered area, the maximum is reached when the snow coverage is already reduced and while temperatures are still rising. The highest temperatures cannot produce extreme snowmelt volumes since the snow-covered area has diminished in the meantime.

A different runoff pattern is obtained from a snow lysimeter with a surface area of 5 $m^2$. The snow coverage was 100% until the last few days. Consequently, the outflow from the lysimeter keeps rising and then abruptly ceases.

This example shows the importance of the snow cover monitoring for snowmelt-runoff computations. A realistic input thus obtained must be of course transformed into the output, that is to say into discharge from a mountain basin.

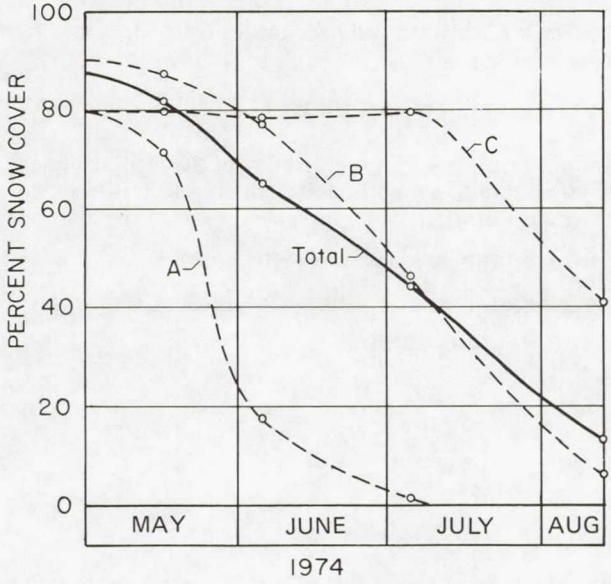


Fig. 4—Depletion curves of the snow coverage in the Dischma basin and in the zones A, B, C, 1974.

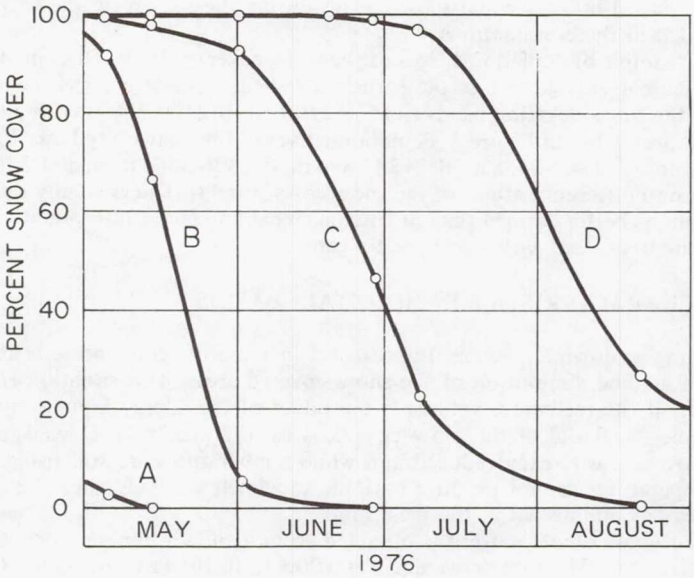


Fig. 5—Depletion curves of the snow coverage in the Dinwoody Creek basin (Rocky Mountains), zones A, B, C, D.

## SNOWMELT-RUNOFF MODEL

A simple relation between daily meltwater production and resulting runoff can be derived as follows:

$$M_1 = R_t = R_1 \frac{k^{\infty} - 1}{k - 1} \tag{1}$$

where $M_1$ is the snowmelt [cm] on the first day of the melting period,
$R_t$ is the total resulting runoff depth [cm] (neglecting losses),
$R_1$ is the runoff depth in 24 hours since the rise of the hydrograph [cm],
$k = \frac{R_m}{R_{m-1}}$ is the recession coefficient.
m refers to a sequence of days during recession.

Since $k < 1$, it follows that:

$$M_1 = R_t = R_1 \frac{1}{1 - k} \tag{2}$$

and

$$R_1 = M_1 (1 - k) \tag{3}$$

On the nth day,

$$R_n = M_n (1 - k) + R_{n-1} \cdot k \tag{4}$$

The superimposition of the immediate meltwater contribution on the extrapolated recession curve is illustrated in Figure 7.

Daily snowmelt depths are determined by the degree-day method:

$$M = a \cdot T \tag{5}$$

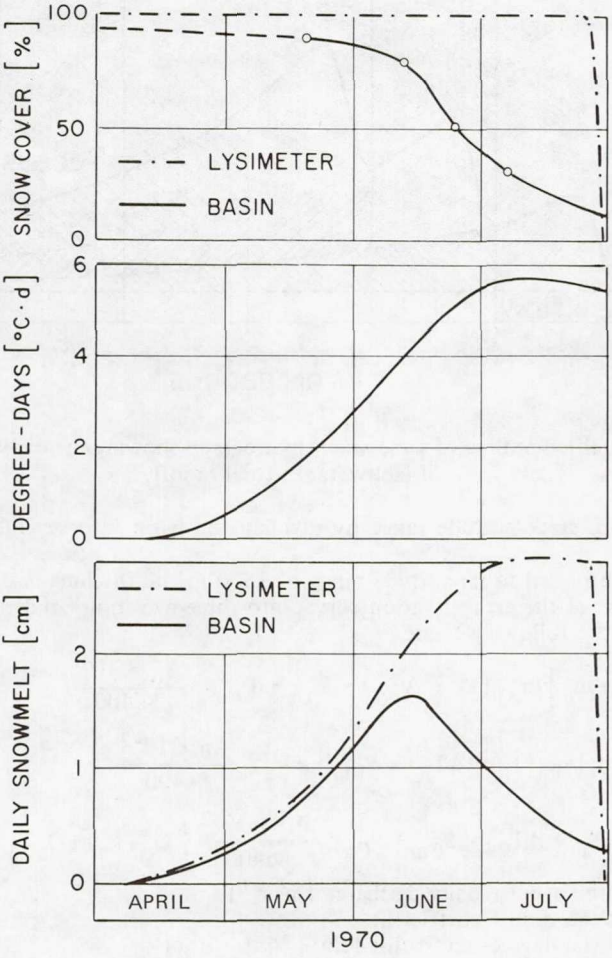


Fig. 6–Effect of depletion curves of snow coverage on runoff patterns in a basin and on a snow lysimeter.

where M is the daily snowmelt depth [cm],
a is the degree-day factor [cm · $°C^{-1}$ · $d^{-1}$],
T is the number of degree-days [°C · d]

This simple relation could be refined by taking into account the whole energy balance. However, if a snowmelt runoff model can perform well with temperature data only, there are better prospects of practical applications.

The so called "Martinec model" [Martinec, 1970] has been developed with the characteristics of snowmelt-runoff in mountain basins in mind, without attempting to achieve a universal validity. It is based on monitoring the areal extent of the snow cover and on a proper assessment of the recession coefficient. It can be

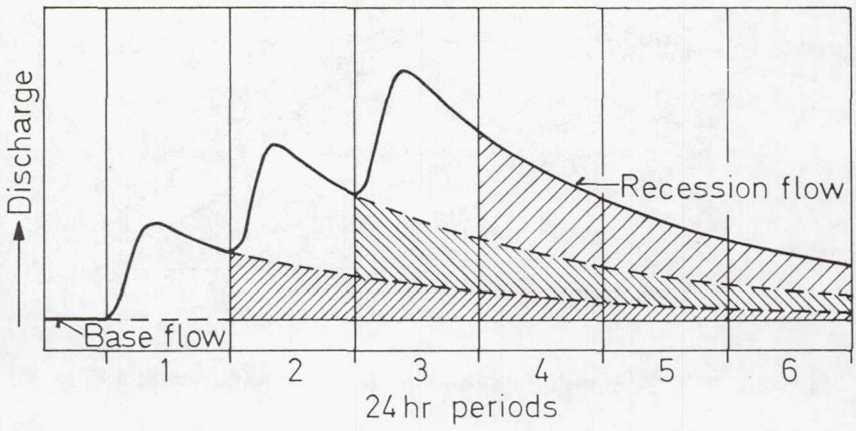


Fig. 7—Simplified outline of a snowmelt hydrograph showing the daily contribution of meltwater to total runoff.

adapted to a great altitude range by dividing the basin into several elevation zones.

With regard to its altitude range of 1500 m, the Dischma basin was divided, with the use of the area-elevation curve, into three elevation bands. The model then takes the following form:

$$Q_n = c_n \Big\{ [a_{An}(T_n + \Delta T_A) \cdot S_{An} + P_{An}] \frac{A_A \cdot 10^{-2}}{86400} + [a_{Bn}(T_n + \Delta T_B) \cdot S_{Bn} + P_{Bn}] \frac{A_B \cdot 10^{-2}}{86400} + [a_{Cn}(T_n + \Delta T_C) \cdot S_{Cn} + P_{Cn}] \frac{A_C \cdot 10^{-2}}{86400} \Big\} (1 - k_n) + Q_{n-1} \cdot k_n \quad (6)$$

where Q is the average daily discharge [$m^3 s^{-1}$]
$c_n$ is the runoff coefficient
$a_n$ is the degree-day factor [$cm \cdot °C^{-1} \cdot d^{-1}$]
$T_n$ is the measured number of degree-days [$°C \cdot d$]
$\Delta T$ is the correction by the temperature lapse rate [$°C \cdot d$]
S is the snow coverage (100% = 1.0)
$P_n$ is the precipitation contributing to runoff [cm]
A is the area [$m^2$]
$k_n$ is the recession coefficient
n is an index referring to the sequence of days
A, B, C as indices refer to the three elevation zones
$\frac{10^{-2}}{86400}$ converts $cm \cdot m^2$ per day to $m^3 s^{-1}$

The recession coefficient appears to be variable, depending on the current discharge by a function:

$$k = x \cdot Q^{-y} \quad (7)$$

The factors x, y must be determined for the given watershed. For example, each daily discharge $Q_n$ can be plotted against the subsequent discharge $Q_{n+1}$. From

the envelope of points indicating a decreasing runoff, it is possible to determine k for any desired Q and to evaluate x, y. If discharge data are not available, the size of the basin might be of assistance to estimate the relation between k and Q.

Since direct measurements of the degree-day factor are seldom available, an empirical relation [Martinec, 1960] may be of assistance:

$$a\ [\text{cm} \cdot {}^{\circ}\text{C}^{-1}\text{d}^{-1}] = 1.1\frac{\rho_s}{\rho_w} \qquad (8)$$

where $\rho_s$ and $\rho_w$ are the density of snow and water, respectively. This equation is not valid for ice.

The model can be tested by comparing the computed values with the measured discharge data.

## RESULTS OF THE RUNOFF SIMULATION

Figure 8 shows a comparison of day-to-day computations by equation (6) with the measured discharge in the Dischma basin. The numbers of degree-days were determined for 24 hour periods starting at 0600 hours. With regard to the time-lag, the corresponding discharge values refer to 24 hour periods starting at 1200 hours. The simulation started on 8 May by computing $k_{8.5} = 0.87$ from the

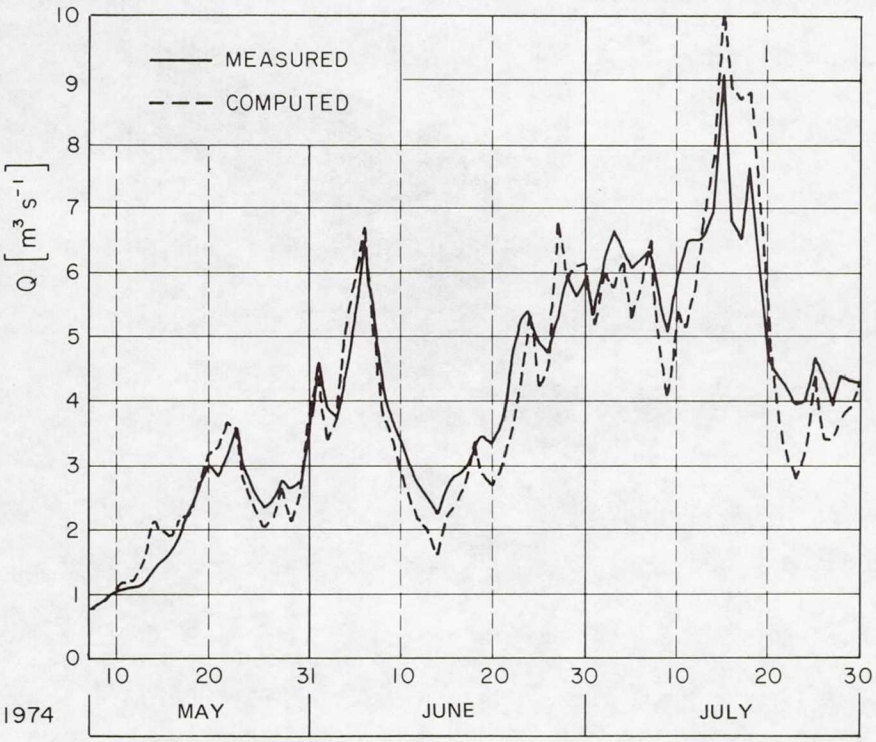


Fig. 8—Computed and measured runoff in the Dischma basin in the snowmelt season 1974.

measured $Q_{7.5} = 0.77\ m^3s^{-1}$ by equation (7) with x = 0.85, y = 0.086. From then on, only computed Q was used until 30 July to determine the next day's value of k. The degree-day ratios were obtained by equation (8) from snow density measurements and varied from 0.45 to 0.55. A uniform temperature lapse-rate of 0.65°C per 100 m altitude difference was used for extrapolations of degree-days to the hypsometric mean elevations of the zones A, B, and C. Uncertainties associated with this temperature extrapolation were reduced by an automatic meteorological station placed at the average altitude of the basin. The runoff coefficient c was estimated in the range of 0.9 to 1.0 for snow and by 0.7 for any additional rainfall. The snow coverage was periodically determined from orthophotographs and read off each day from the depletion curves (Figure 4).

Another application in the Dinwoody Creek basin in the Wind River Mountains tested the model in new, less favorable conditions differing from those of a well-equipped representative basin. Only temperature and precipitation data from a station 100 km outside the basin, as well as snow-cover images from Landsats 1 and 2 were available for computing the snowmelt runoff. An example of Dinwoody Creek snow cover as viewed from Landsat is shown in Figure 9.

In view of the altitude range of over 2000 m on the Dinwoody basin, the model formula was extended to four elevation bands. A time-lag of about 18 hours was estimated from discharge records. This value is at least partially explained by

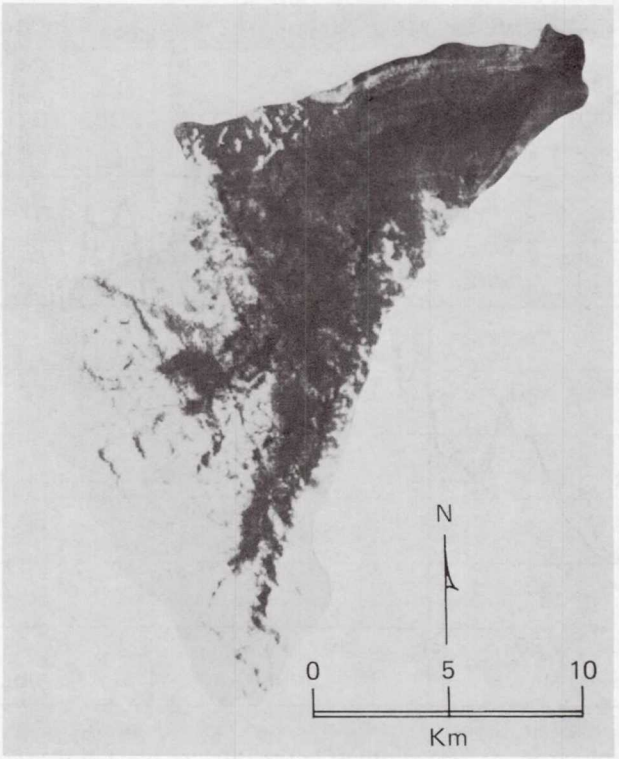


Fig. 9—Landsat image of the Dinwoody Creek basin on 28 June 1976.

the greater size of the basin as compared with the previous case. Equation (6) was thus rearranged as follows:

$$Q_{n+1} = c_n (I_{An} + I_{Bn} + I_{Cn} + I_{Dn}) (1 - k_{n+1}) + Q_n k_{n+1} \quad (9)$$

where the inputs I are again:

$$I_{Nn} = [a_{Nn} (T_n + \Delta T_N) \cdot S_{Nn} + P_{Nn}] \frac{A_N \cdot 10^{-2}}{86400} \quad (10)$$

By analyzing Dinwoody discharge data from 1973 to 1976, x = 0.884 and y = 0.0677 were derived for determining k by equation (7).

The simulation started on April 1, 1976 by computing $k_{2.4}$ from the measured $Q_{1.4}$ to compute $Q_{2.4}$. Afterwards, for the 6-month period, the computed Q was always used to determine the next k. No updating was thus carried out. In view of the length of the period, seasonal variations of losses and of the temperature lapse rate were taken into account on the basis of available information about the climate [Barry and Chorley, 1970]. The runoff coefficient was estimated in the range from 0.85 in April to 0.75 in July to 0.9 in September. The temperature lapse rate appeared to be higher than in the Alps. Values varying from 0.85°C per 100 m in April to 0.95°C per 100 m in July and 0.80°C per 100 m in September were used. In addition, regional differences between the meteorological station at Lander airport and the basin were accounted for by subtracting up to 2°C from the Lander data.

The degree-day factor was assessed in the range from 0.35 at the start to 0.6 at the end of the snowmelt season. The delay of the snow ripening in the high parts of the basin was taken into account by differentiating the degree-day ratios in the respective elevation zones. The snow coverage was determined each day from the depletion curves shown in Figure 5.

With all variables and parameters of the model thus measured or determined, tables have been prepared for the numerical and graphical evaluation according to Equations (9, 10). While S, k, T, P are changing each day, a, c, $\Delta T$ are adjusted stepwise in intervals of several weeks or months.

The comparison of the simulated runoff with discharge measurements of the U.S. Geological Survey illustrated in Figure 10 shows a reasonable agreement. A number of the deviations seem to have been caused by the insufficient precipitation data.

Adequate Landsat data from the year 1974 provided another opportunity for a snowmelt-runoff simulation in the Dinwoody Creek basin. Seasonal changes of of the temperature lapse rate, of the runoff coefficient, and of the degree-day factor were again varied as in 1976 for this basin. Judging from the depletion curves of 1974, the progress of the snowmelt season seemed to be accelerated by about 2 weeks in comparison with 1976. In an attempt to take this roughly into account, the seasonal course of the runoff coefficient, of the temperature lapse rate, and of the degree-day factor was generally shifted in a corresponding sense. Figure 11 shows again a good agreement between the simulated and measured runoff for 1974.

Since the measured discharge was never used for an updating, it seems possible to simulate discharge in ungaged sites by using Landsat images of the snow cover together with temperature and precipitation data.

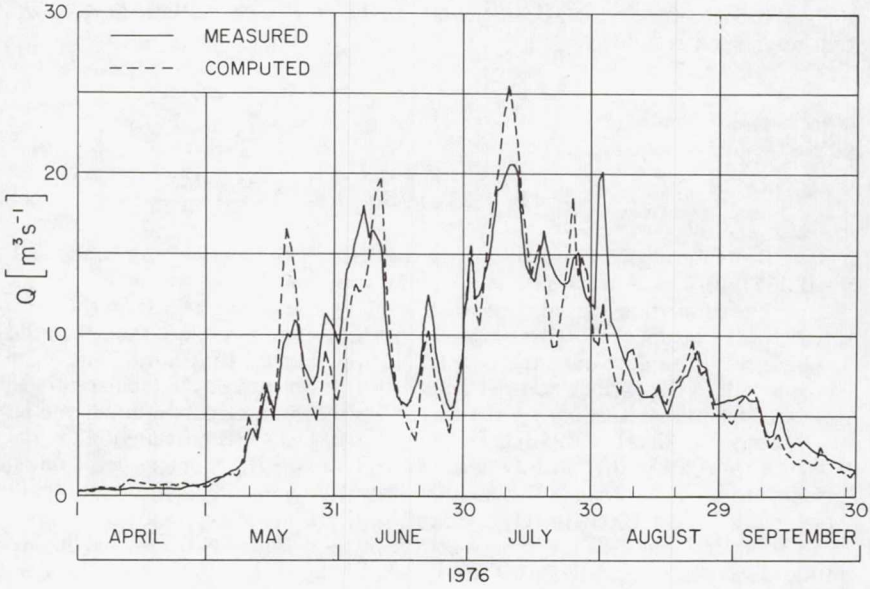


Fig. 10–Computed and measured runoff in the Dinwoody Creek basin in the summer half year 1976.

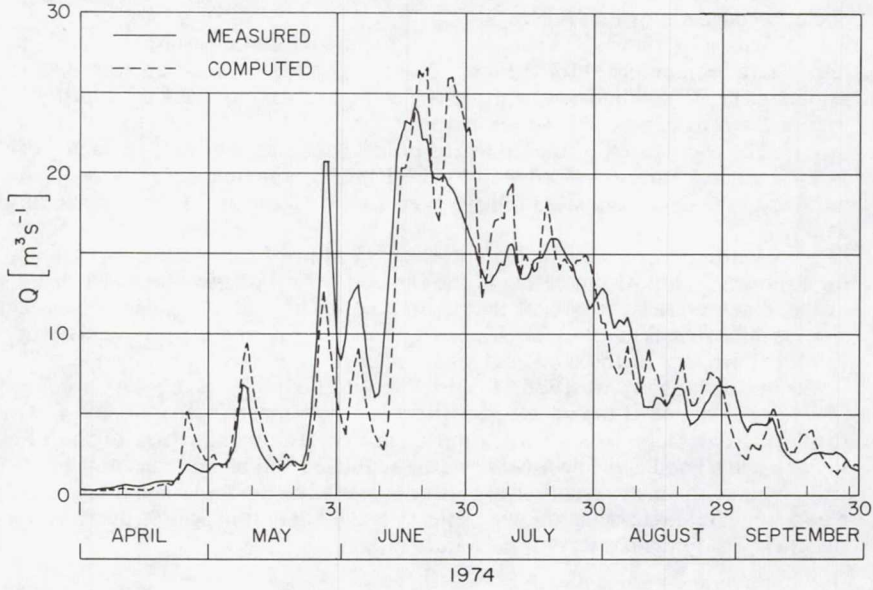


Fig. 11–Computed and measured runoff in the Dinwoody Creek basin in the summer half year 1974.

## APPLICATION TO OTHER AREAS; DISCHARGE FORECASTS

In order to be useful for operational hydrology, satellite snow-cover monitoring must satisfy certain requirements, primary of which are frequency of coverage, spatial resolution, and timeliness of data. Although the snowmelt model can provide daily runoff forecasts, it is not necessary to observe the snow cover on a daily basis. Rather, in the Wind River Mountains it appears that because of favorable cloud cover conditions during the snowmelt period, satellite coverage of once every nine days (as provided with the 80 m resolution data from the two Landsat vehicles) is nearly adequate for runoff forecasting purposes. When cloud cover frequency increases (as shown in Figure 12), however, more frequent satellite coverage is also required, perhaps as much as once every 1-3 days. In the future in extremely cloudy areas it may even be necessary to switch from visible to high resolution microwave sensors that can penetrate clouds. Timeliness of data is essentially an information management problem which can be solved as the required satellite systems become operational. It appears that a realistic goal for delivery of the snow-cover data for operational purposes is within 72 hours after data acquisition.

To facilitate a determination of where Landsat capabilities would be appropriate for snow-cover monitoring and daily runoff forecasts, cloud cover statistics for Landsat overpasses were generated for the Wind River Mountains of Wyoming (considered a marginally useable area) and then compared with statistics from other

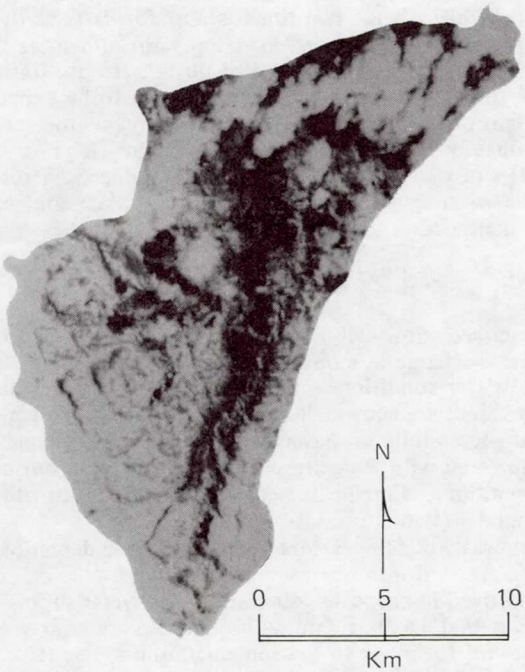


Fig. 12—Landsat image of the Dinwoody Creek basin showing snow cover with clouds on 10 June 1976.

important snowmelt runoff areas in the western United States. The cloud cover for each Landsat image obtained during the April – September snowmelt period was categorized as a percent (%) rounded off to the next highest increment of 10 for 1973–1978. Assuming that Landsat scenes with 40% or less cloud cover are useable for snow-cover delineation, approximately 73% of all Landsat passes over the Wind River Mountains during the snowmelt period will provide meaningful snow-cover information. This compares to 81% in the White Mountains of central Arizona, 91% in the southern Sierra Nevada Mountains of California, 81% in the San Juan Mountains of Colorado, and 55% in the northern Rocky Mountains of Montana. Based on these comparisons it appears that Landsat-type operational snow-cover data would be useful for snowmelt runoff simulations and perhaps forecasts in several important snowmelt runoff zones in the western United States, with the major difficulty being experienced in the northern Rocky Mountains and coastal ranges of the northwest United States where an increased frequency of cloudiness as well as heavy timber cover limits unobstructed Landsat views. More frequent coverage as well as cloud penetrating microwave capabilities will probably be necessary in this important snow zone of the northwest United States.

Cloud cover data for other mountain ranges around the world is incomplete and comparisons cannot be made. It is known, however, that significant cloud cover problems exist in the Alps that mandate improvements over the current Landsat system before snowmelt-runoff forecasts can be made.

Naturally, a runoff simulation from a past season for which all data are available is not a forecast. However, this simple model needs only temperatures and the snow coverage. While real time data or forecasts of the energy budget are difficult to obtain (Limpert, 1975), temperature forecasts for several days in advance are frequently available. It is also possible to use statistical temperature data to predict the maximum and minimum runoff to be expected in a given period with a certain probability. The depletion curves of the snow-covered areas can be approximately extrapolated and up-dated by each new satellite observation. The uncertainties of this extrapolation could be reduced by research into the relation of the snow-cover depletion curves to the initial water equivalent of the snowpack and melt-period temperatures.

## CONCLUSIONS

The described snowmelt-runoff model together with Landsat data can be used to simulate discharge in mountainous areas with a large elevation range and moderate cloud cover conditions (cloud cover of 40% or less during Landsat passes 70% of the time during a snowmelt season). So far the snowmelt-runoff model has been tested successfully on basins with areas not exceeding several hundred square kilometers and with a significant component of subsurface runoff. For different basin conditions, it might be necessary to emphasize additional factors in such a runoff model (Hannaford, 1977).

With forecasts of temperature and snow-cover depletions, the model simulations can be converted into operational discharge forecasts. The forecasts would be used for improved hydropower generation and water supply allocations.

It appears that Landsat data with once every nine day coverage would be operationally useful for input to the snowmelt-runoff model in mountainous portions of Wyoming, Colorado, the arid Southwest, and southern California in the United States. Cloud cover in the northern Rocky Mountains and the coastal ranges of the northwest United States markedly reduces the effectiveness of Landsat, however.

In regions where cloud cover frequency limits the usefulness of the current Landsat system, several alternative solutions should be considered for the future: evolution of an operational Landsat system with coverage available at least once every three days; the use of synchronous satellite data with a resolution of 1 km or less; operational aircraft coverage; or development of a high resolution microwave system for penetrating the clouds. Any of these systems should facilitate obtaining the important snow cover input data for use in snowmelt-runoff forecasts.

## ACKNOWLEDGMENTS

We would like to thank H. J. Etter, G. Klausegger, J. V. Niederhäusern, and E. Wengi, Federal Institute for Snow and Avalanche Research, James L. Foster, Goddard Space Flight Center, and Ralph Peterson, General Electric Company, Beltsville, Maryland, U.S.A. for performing essential data analysis for this project. Necessary data were supplied by the U.S. Geological Survey, U.S. Soil Conservation Service, and the National Oceanic and Atmospheric Administration. Special gratitude is extended to the Director of the Federal Institute for Snow and Avalanche Research, Prof. M. de Quervain, and to the Acting Director of Applications, Goddard Space Flight Center, Dr. L. Meredith for their continuing support of this international cooperation.

## REFERENCES

Barry, R. G., and R. J. Chorley, Atmosphere, Weather and Climate, Holt, Rinehart, and Winston, Inc., New York, 320 pp., 1970.

Haeffner, A. D., and A. H. Barnes, Photogrammetric determinations of snow cover extent from uncontrolled aerial photographs, American Society of Photogrammetry, Technical Session Proceedings, Columbus, Ohio, pp 319-340, October, 1972.

Hannaford, J. F., Investigation application of satellite imagery to hydrologic modeling snowmelt runoff in the southern Sierra Nevada, Phase 1 Final Report, NAS 5-22957, NASA, Goddard Space Flight Center, Greenbelt, Maryland, 48 pp., 1977.

Leaf, C. F., Aerial photographs for operational streamflow forecasting in the Colorado Rockies, Proceedings of the 37th Annual Western Snow Conference, Salt Lake City, Utah, pp. 19-28, 1969.

Limpert, F. A., Operational application of satellite snowcover observations – northwest United States, Proceedings of the Workshop on Operational Applications of Satellite Snowcover Observations, NASA SP-391, Washington, D.C., pp. 71-85, 1975.

Martinec, J., The degree-day factor for snowmelt-runoff forecasting, IAHS Publication No. 51, Surface Waters, pp. 468-477, 1960.

Martinec, J., Study of snowmelt-runoff process in two representative watersheds with different elevation range, IAHS Publication No. 96, Symposium of Wellington (N.Z.), pp. 29-39, 1970.

Martinec, J., Evaluation of air photos for snowmelt-runoff forecasts, Proceedings of the Banff Symposium – The Role of Snow and Ice in Hydrology, IAHS – AISH Publication No. 107, pp. 915-926, 1972.

Rango, A., Remote sensing: snow monitoring tool for today and tomorrow, Proceedings of the 45th Annual Western Snow Conference, Albuquerque, New Mexico, pp. 75-81, 1977.

Urfer, H. P., Routinemässige Schneekartierungen in hydrologischen Einzugsgebieten (Routine snow mapping in hydrologic basins), M. Sc. Thesis, Department of Geography, University of Zurich, 1978.

Warskow, W. L., T. T. Wilson, and E. Kirdar, The application of hydrometeorological data obtained by remote sensing techniques for multipurpose reservoir operations, Proceedings of the Workshop on Operational Applications of Satellite Snowcover Observations, NASA SP-391, Washington, D.C., pp. 29–37, 1975.